Theoretical modeling of two-step spin-crossover transitions in Fe^{II} dinuclear systems

Jordi Cirera and Eliseo Ruiz

Departament de Química Inorgànica and Institut de Recerca de Química Teòrica i Computacional, Universitat de Barcelona, Diagonal 645, 08028 Barcelona, Spain

Email corresponding authors: eliseo.ruiz@qi.ub.es; jordi.cirera@qi.ub.es

Abstract

A computational methodology to model the spin-transition in the dinuclear iron(II) systems $[Fe(bt)(NCX)_2]_2(\mu\text{-bpym})$ and $[Fe(pypzH)(NCX)]_2(\mu\text{-pypz})_2$ (X = S, Se or BH_3) is presented. Using the hybrid meta-GGA exchange-correlation functional TPSSh, accurate values for the thermochemical quantities associated with the different spin-states can be computed, and subsequently used to calculate the corresponding transition temperatures. This results also allow for the correct modeling of the spin-crossover curve, in agreement with the two-step or single-step nature experimentally reported for the transition. Our results indicate that the presence or absence of a two-step transition is mostly dominated by electronic effects and cooperativity between binding pockets plays a minor role. Insight in the electronic structure effects that enhance or suppress this behavior and its origins can be outlined from direct analysis of the relevant d-based molecular orbitals, which allows for a quantitative computational prediction to screen for new dinuclear systems with selected properties.

Keywords: Spin-Crossover, Density Functional Theory, Transition Temperature, dinuclear iron(II) complexes.

1. Introduction

Spin-Crossover (SCO) systems have been the focus of intense research in several scientific fields due to their intrinsic physical properties as molecular level switches. Since the first Fe^{III} spin-crossover molecules were reported by Cambi and co-workers in 1931,[1] the number of systems exhibiting spin-crossover has significantly grown and expanded to other coordination numbers, metal centers and oxidation states, and it has also been reported for systems with increasing nuclearity. This phenomena has been extensively covered in the literature,[2-7] and spin-crossover systems continue providing with new and more sophisticated examples and applications, such as its incorporation in metal-organic frameworks for the design of spin-crossover materials. [8-13]. The spin-crossover phenomenon may appear in systems in which states with different spin have similar electronic energies. In such cases, entropy favors the high-spin state and a transition from the low-spin state, observed at low-temperature, to the high-spin state, dominant at higher temperatures can be observed.[2] Although thermal spin-crossover is by far the most studied way of inducing the transition, spin-crossover can be also controlled by means of external pressure, electromagnetic radiation (light) and electric fields.[2, 14] Because the spin transition involves significant rearrangements in the electronic structure of the metal center, major changes in the physical properties of these molecules are observed upon the transition occurs. Such changes include different magnetic moments, changes in the electronic spectrum and sensible changes in the coordination geometry. It is precisely this fact what makes spin-crossover systems perfect candidates for actual technological applications in molecular level data storage systems or nanoscale sensing devices.[14-18]

An intermediate point between mononuclear spin-crossover systems and spin-crossover frameworks can be found in polymeric complexes including two or more metal centers able to undergo a spin transition. In these systems, the strong interaction between metal centers can lead to a higher cooperativity, which can in turn make the spin transition sharper, a highly pursued characteristic in order to use these systems in actual technological applications. Among the polynuclear SCO reported systems, dinuclear iron(II) complexes are the most widely studied, and its number has been steady growing over the last years.[2, 8, 19-21] A key feature in these molecules is the presence or absence of a two-step transition, this is, the possibility that the transition occurs via a ”mixed” high-spin/low-spin [HS-LS] state. This intermediate spin-state has been experimentally characterized using magnetic and structural data as well as Mössbauer spectroscopy for several dinuclear complexes.[8] Although few experimental rules have been outlined in order to predict a transition via a localized [HS-LS] state, such as the use of highly constrained ligands.[22-24] It is still hard to foresee which systems will undergo spin-crossover in one-step and which ones will do it via a two-step mechanism. It has been proposed though, that the stability of the [HS-LS] spin-state can be related with the decrease in the enthalpy change with respect to the halfway point between the total enthalpy change for the transition from the low-spin/low-spin [LS-LS] state to the high-spin/high-spin [HS-HS] state.[25-27] Although strong intermolecular interactions can indeed play a role in shaping the transition, the intramolecular interactions usually play a major role in controlling the stability of the intermediate [HS-LS] species.

Mononuclear spin-crossover systems have been successfully characterized over the last years using electronic structure calculations at Density Functional Theory (DFT) level.[28-32] Among them, the meta-hybrid GGA functional TPSSh[33, 34]

seems to be the method of choice due to their unprecedented balance between accuracy and computational cost. This DFT method has been previously described, and successfully used to characterize thermochemical quantities in mononuclear spin-crossover systems, as well as transition temperatures and the effects that chemical changes on the ligand field around the metal center have over the $T_{1/2}$.[35-38] In this work, we present our results for the electronic structure modeling of dinuclear Fe^{II} systems, [Fe^{II}-Fe^{II}], for which experimental data showing a two-step transition or a single step-transition has been experimentally reported. In particular, our results for the $[Fe(bt)(NCS)_2]_2(\mu\text{-bpym})$ and $Fe(pypzH)(NCSe)]_2(\mu\text{-pypz})_2$ systems will be presented, for which experimental structural and magnetic data is available.[25, 39] Further insight on the origin and stability of the two-step feature can be obtained by exploring the effect that tuning the ligand field around the metal center produces on the stability of the [HS-LS] intermediate spin-state. We will also present our results for the corresponding expanded families $[Fe(bt)(NCX)_2]_2(\mu\text{-bpym})$ and $Fe(pypzH)(NCX)]_2(\mu\text{-pypz})_2$ (X = S, Se and BH_3), for which increasing ligand fields introduce a progressive destabilization on the intermediate spin-state. The article is organized as follows: In section 2, the computational methodology is described, while the results are discussed in section 3. The discussion is given in section 4 and finally the conclusions will be presented.

2. Methodology

2.1. Computational methods

All Density Functional Theory (DFT) calculations were carried out with Gaussian 09 (revision D.01)[40] electronic structure package with a 10^{-8} convergence criterion for the density matrix elements, using the hybrid-meta GGA functional

TPSSh.[33, 34] This functional has been previously used with success in the modeling of accurate thermochemical quantities for several mononuclear Fe^{II} spin-crossover systems.[35, 36] The fully optimized contracted triple-ζ all electron Gaussian basis set developed by Ahlrichs and co-workers was employed for all the elements with polarization functions being added on the Fe center.[41] The different spin topologies were modeled using the fragments option, which allows the definition of specific electronic structures for each metal center. For all the studied dinuclear systems, we fully optimized the molecules in all possible spin configurations ([HS-HS], [HS-LS] and [LS-LS]) and performed the subsequently vibrational analysis, which later can be used to compute the thermochemical quantities (see ESI for optimized structures).

2.2. Modeling SCO in dinuclear systems

To model the transition temperature in dinuclear Fe^{II} spin-crossover systems, we used the fact that spin-crossover phenomena can be described as a thermodynamic equilibrium between the fully high spin ([HS-HS]) and the fully low-spin ([LS-LS]) states. This transition can occur via two different pathways: a one-step transition, from the [LS-LS] to the [HS-HS] state, or a two-step transition, involving the intermediate [HS-LS] state. The Gibbs free energy change associated with this process is summarized in [1].

$$[\text{LS-LS}] \leftrightarrows [\text{HS-LS}] \leftrightarrows [\text{HS-HS}] \qquad [1]$$

Assuming and ideal system, in which the spin-crossover system is isolated, and due to the fact that the pressure-dependent term to the free enthalpy change is usually small, we can write the corresponding free energy changes for each process (ΔG) for the equilibrium expression of [1] as,[42, 43]

$$\Delta G = G^{S_1} - G^{S_2} = \Delta H - T\Delta S \qquad [2]$$

where

$$G^i = H^i - TS^i = E^i_{el} + E^i_{vib} - TS^i \qquad [3]$$

is the Gibbs free energy associated with spin state *i* (ie., [HS-HS], [HS-LS] or [LS-LS] at a given temperature. In equation [3], the enthalpy term (H^i) includes both electronic (E^i_{el}) and vibrational (E^i_{vib}) contributions. For molecular complexes, E^i_{vib} can be properly estimated by using the harmonic approximation, while the term E^i_{el}, describing the electronic energy of spin state *i*, can be obtained directly from *ab initio* calculations. The entropy contribution to the free energy (S^i) can also be estimated using the harmonic approximation.

Given that the Gibbs free energy is a state function, the total change in the free energy between the [HS-HS] and the [LS-LS] states, ΔG_T, must be equal to the free energy changes between the [HS-HS] and [HS-LS] states (ΔG_1) plus the free energy change between the [HS-LS] and [LS-LS] states (ΔG_2). Therefore, we can use the individual equilibrium constants K_1 and K_2, to write down the corresponding molar fractions of each spin-states as follows,

$$\Delta G_i(T) = -RT \ln K_i = -RT \ln \frac{\gamma_{S_1}}{\gamma_{S_2}} = -RT \ln \frac{\gamma_{S_1}}{1-\gamma_{S_1}} \qquad [4]$$

Equation [4] can be recast so the molar fraction of the corresponding spin-state depends on the change in the free energy at each temperature as,

$$\gamma_{S_1}(T) = \left[1 + e^{\Delta G_i(T)/RT}\right]^{-1} \qquad [5]$$

where *R* is the gas constant and *T* the temperature. It is worth mentioning that both ΔH and ΔS have some temperature dependence that can be, in principle, be neglected without loosing accuracy.

3. Results

For this work, we have chosen two dinuclear systems well characterized from the structural and electronic point of view (Fig. 1), the $[Fe(bt)(NCS)_2]_2(\mu\text{-bpym})$ and $[Fe(pypzH)(NCSe)]_2(\mu\text{-pypz})_2$ molecules.[25, 39] The former displays a two-step transition, while the latter displays a sharp one-step transition. Geometry optimizations for all the studied systems were calculated in all possible spin-configurations, and compared with the experimental data when available. As it is well know, spin-crossover produces significant changes in the metal-ligand bond lengths, effect that is directly related to the different electronic structures of the metal centers in each spin-state. For and iron(II) (d^6), in the low-spin state, only the non-bonding set of orbitals (d_{xz},d_{yz} and d_{xy}) is occupied, while in the high-spin state occupation of the antibonding $d_{x^2-y^2}$ and d_{z^2} orbitals leads to a significant enlargement of the metal-ligand bond lengths. All our calculations are in good agreement with the experimental information, which is key in correctly reproducing the SCO behavior for the studied systems. A whole list of bond lengths and bond angles can be found in the Supporting Information (ESI).

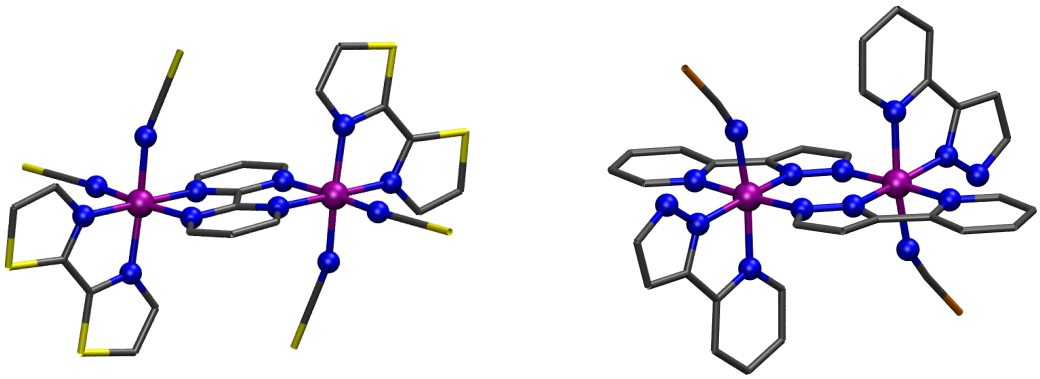

$[Fe(bt)(NCS)_2]_2(\mu\text{-bpym})$ $[Fe(pypzH)(NCSe)]_2(\mu\text{-pypz})_2$

Fig. 1 Molecular representations for the iron(II) dinuclear systems studied in this work. (bt = 2,2'-bi-2-thiazoline, bpym = 2,2'-bipyrimidine, pypzH = 2-pyrazolylpyridine). Hydrogen atoms omitted for clarity. Color scheme: Fe (purple), C (grey), N (blue), S (yellow) and Se (orange).

It has been previously reported that the presence or absence of a two-step transition can be related with the energy stabilization of the [HS-LS] spin-state relative to the halfway point of the total enthalpy change between the [HS-HS] to the [LS-LS] states. In particular, if the enthalpy change between the [HS-LS] and the [LS-LS] states is lower than the halfway point between the enthalpy change between the [LS-LS] to the [HS-HS] states, or if the difference in enthalpies is tiny but strong intermolecular interactions are present, then SCO can occur through a two-step transition.[25-27] Intramolecular interactions responsible for the stabilization of the [HS-LS] state can be characterized by the parameter ρ (ρ = W/ΔH),[25-27] defined as the ratio between the energetic stabilization of the [HS-LS] state relative to the halfway point between the enthalpy change for the [HS-HS] to the [LS-LS] transition (W) and this same enthalpy change (ΔH) (see Fig, 2). Negative values of ρ are associated with a more favorable situation in terms of displaying a two-step transition, while positive values will be indicative of a single step transition.

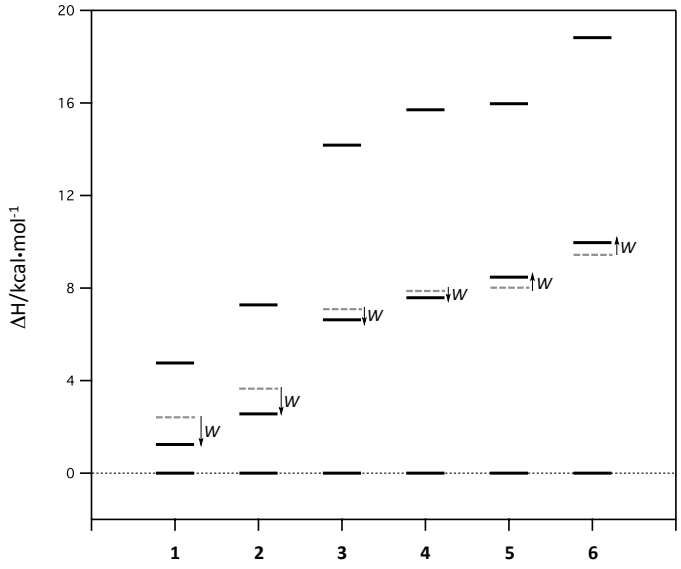

Fig. 2 Calculated enthalpy changes for the spin-states [HS-HS], [HS-LS] and [LS-LS] for the systems $[Fe(bt)(NCX)_2]_2(\mu\text{-bpym})$ and $[Fe(pypzH)(NCX)]_2(\mu\text{-pypz})_2$ where X = S, Se and BH_3. Dashed line corresponds to the halfway point on the enthalpy change between the [HS-HS] and the [LS-LS] states. *x*-axis labeling correspondence in Table 1.

Table 1 Calculated enthalpy change between the [HS-HS] and [LS-LS] states for the $M_n[Fe_2]$ systems (ΔH), energy stabilization of the [HS-LS] state with respect to $\Delta H/2$ (W), and the corresponding ρ parameter.

System	ΔH/kcal•mol^{-1}	W/kcal•mol^{-1}	ρ
(**1**) $[Fe(bt)(NCS)_2]_2(\mu\text{-bpym})$	4.760	-1.141	-0.240
(**2**) $[Fe(bt)(NCSe)_2]_2(\mu\text{-bpym})$	7.272	-1.074	-0.148
(**3**) $[Fe(bt)(NCBH_3)_2]_2(\mu\text{-bpym})$	15.223	-0.983	-0.065
(**4**) $[Fe(pypzH)(NCS)]_2(\mu\text{-pypz})_2$	15.705	-0.270	-0.017
(**5**) $[Fe(pypzH)(NCSe)]_2(\mu\text{-pypz})_2$	15.966	+0.488	+0.031
(**6**) $[Fe(pypzH)(NCBH_3)]_2(\mu\text{-pypz})_2$	18.823	+0.550	+0.029

As can be seen from the above results, the $[Fe(bt)(NCS)_2]_2(\mu\text{-bpym})$ molecule (**1**) displays the largest stabilization of the [HS-LS] spin-state. By using the corresponding changes in the free energies, as discussed above, a distribution of the

different molar fractions for the different spin-states species can be extracted and used to construct the corresponding curve for the change in the magnetic moment as a function of the temperature (Fig. 3). From the molar fraction plots one can easily extract the corresponding transition temperatures, defined as the temperatures with equal populations of two different spin-states. This temperatures have been computed to be $T_{1/2}(1)$ = 30 K (transition from [LS-LS] to [HS-LS]) and $T_{1/2}(2)$ = 220 K (transition from [HS-LS] to [HS-HS]), in fair agreement with the experimentally reported ones ($T_{1/2}(1)$ = 163 K and $T_{1/2}(2)$ = 197 K).[25] Achieving accuracy in the calculation of transition temperatures is still a challenging problem for DFT calculations, and we must be emphasize here that the TPSSh functional has not been parameterized specifically for transition metal systems, and although its performance is remarkable, some differences with respect to the experimental values must be expected.

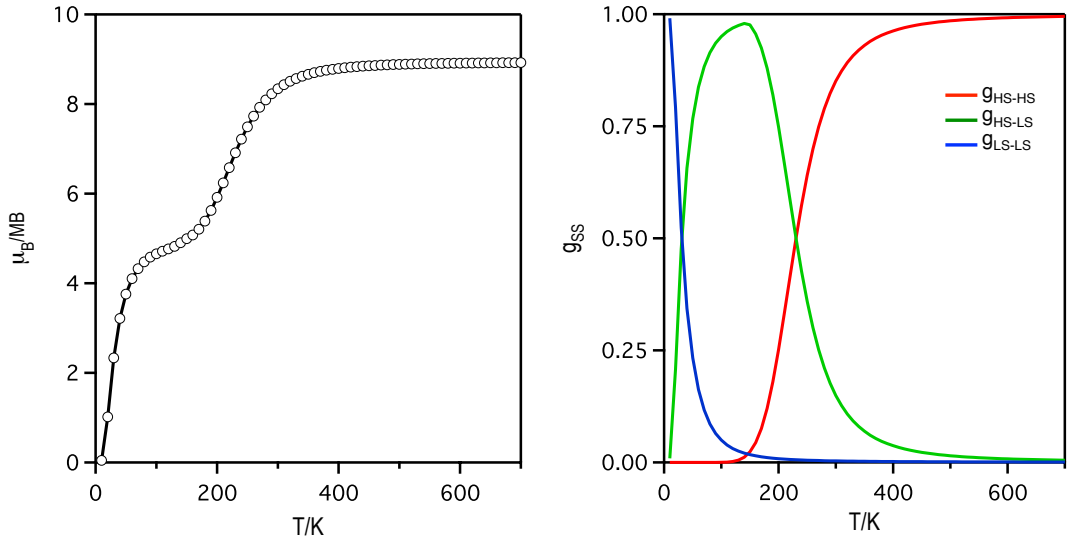

Fig. 3 Calculated magnetic moment for the $[Fe(bt)(NCS)_2]_2(\mu\text{-bpym})$ system (left) and relative molar fractions for the different spin topologies. Red for [HS-HS], green for [HS-LS] and blue for [LS-LS] (right). From the intersection points one can extract the corresponding transition temperatures.

The closely related $[Fe(bt)(NCSe)_2]_2(\mu\text{-bpym})$ molecule (**2**),[44] for which accurate EXAFS data has been collected, also displays a two-step transition, but with the corresponding $T_{1/2}$ values shifted towards higher values (table 2). This results are consistent with the increased ligand field around the metal center introduced by the NCSe ligand.[36] Our calculations correctly model the two-step transition, and the shift to higher values, and also provide with a much smoother curve than for the $[Fe(bt)(NCS)_2]_2(\mu\text{-bpym})$ molecule. It is also important to remark that the optimized bond lengths are in excellent agreement with the ones determined by EXAFS spectroscopy (see ESI).

A different situation is experimentally observed for the $[Fe(pypzH)(NCSe)]_2(\mu\text{-pypz})_2$ (**5**), for which a single-step transition centered at 225K has been reported.[39] Calculations for that system agreed with the experimental data and provided us with a calculated $T_{1/2}$ = 425K, with a corresponding ρ value of +0.031 (table 2). Although the computed transition temperature is higher than the experimentally observed one, the correct behavior for the spin-transition is reproduced. As observed in Fig. 4, for that system the molar fraction of [HS-LS] spin-configuration is always inferior to the molar fractions of the [HS-HS] or [LS-LS] species, which makes the system undergo spin-crossover in a single step between this two spin-states without accessing the intermediate spin-state species.

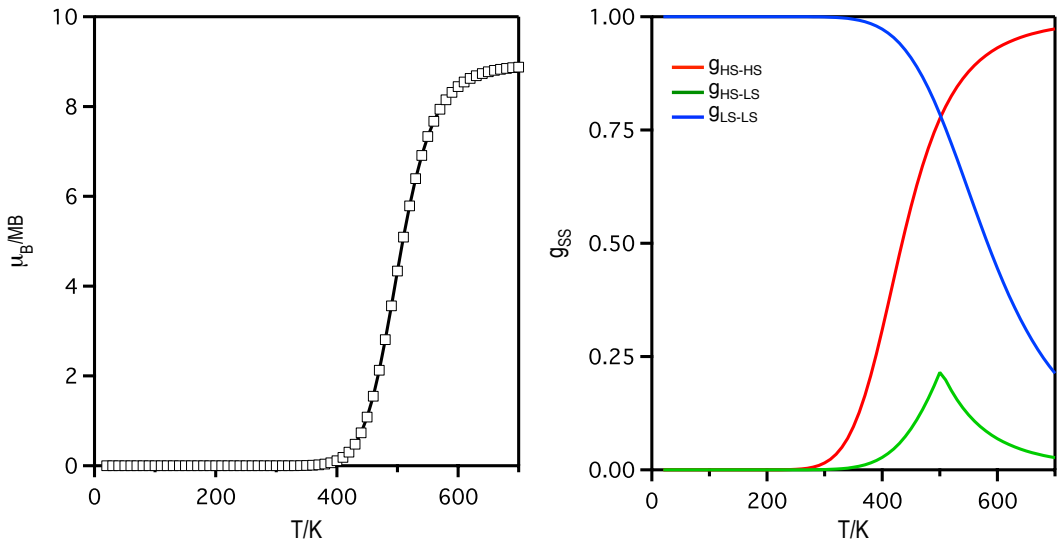

Fig. 4 Calculated magnetic moment for the $[Fe(pypzH)(NCSe)]_2(\mu\text{-}pypz)_2$ complex (4) (left) and relative molar fractions for the different spin topologies. Red for [HS-HS], green for [HS-LS] and blue for [LS-LS] (right). From the intersection points one can extract the corresponding transition temperatures.

Although the current calculations nicely reproduce the experimentally reported data (one-step transition vs. two-step transition), a much more interesting situation arises from the possibility of enhancing or suppressing this behavior via ligand-field tuning. It is very well know that the strength of the ligand field around the metal center in mononuclear spin-crossover systems can be finely tuned by using different members of the NCX family (X = S, Se or BH_3), which progressively increase the strength of the ligand field around the metal center. So, we decided to explore the behavior of the species $[Fe(bt)(NCX)_2]_2(\mu\text{-}bpym)$ and $[Fe(bt)(NCX)_2]_2(\mu\text{-}bpym)$ (X = S, Se and BH_3) to explore the effect of the local ligand field over the intramolecular interactions and its implications in the overall behavior towards spin-crossover. Interestingly, some of these molecules hasn´t been reported yet, which emphasizes the potential use of computational tools for the design of SCO systems with tailored properties. We modeled the X atom from the fully optimized $[Fe(bt)(NCS)_2]_2(\mu\text{-}bpym)$ and $[Fe(bt)(NCSe)_2]_2(\mu\text{-}bpym)$ molecules in both spin-

states and proceed in the same way to calculate the corresponding stabilization energies for the [HS-LS] spin-state species and the corresponding ρ values (table 1). The computed transition temperatures are listed in table 2. It is important to remark here that although the difference between computed and experimental values for the transition temperatures may seem large, the largest error observed in our data set is equivalent to only 0.54kcal/mol. For instance, for the $[Fe(bt)(NCS)_2]_2$(μ-bpym) molecule, the experimentally reported value for the ΔH is 3.16kcal/mol, compared with our 4.76kcal/mol (table 1). These differences, together with the lack of inclusion of intermolecular interactions can be responsible of the observed differences between computed and experimental transition temperatures.

Table 2 Calculated transition temperatures ($T_{1/2}$) for the $[Fe(bt)(NCX)_2]_2$(μ-bpym) and $[Fe(pypzH)(NCX)]_2$(μ-$pypz)_2$ (X = S, Se, BH_3) molecules. Comparison with the experimental values is provided when possible. All temperatures are in K.

System	$T^1_{1/2}$ (calc)	$T^1_{1/2}$ (exp)	$T^2_{1/2}$ (calc)	$T^2_{1/2}$ (exp)
(**1**) $[Fe(bt)(NCS)_2]_2$(μ-bpym)	30	163	235	197
(**2**) $[Fe(bt)(NCSe)_2]_2$(μ-bpym)	155	225	305	262
(**3**) $[Fe(bt)(NCBH_3)_2]_2$(μ-bpym)	385	not reported		
(**4**) $[Fe(pypzH)(NCS)]_2$(μ-$pypz)_2$	455	not reported	-	-
(**5**) $[Fe(pypzH)(NCSe)]_2$(μ-$pypz)_2$	495	225	-	-
(**6**) $[Fe(pypzH)(NCBH_3)]_2$(μ-$pypz)_2$	535	not reported	-	-

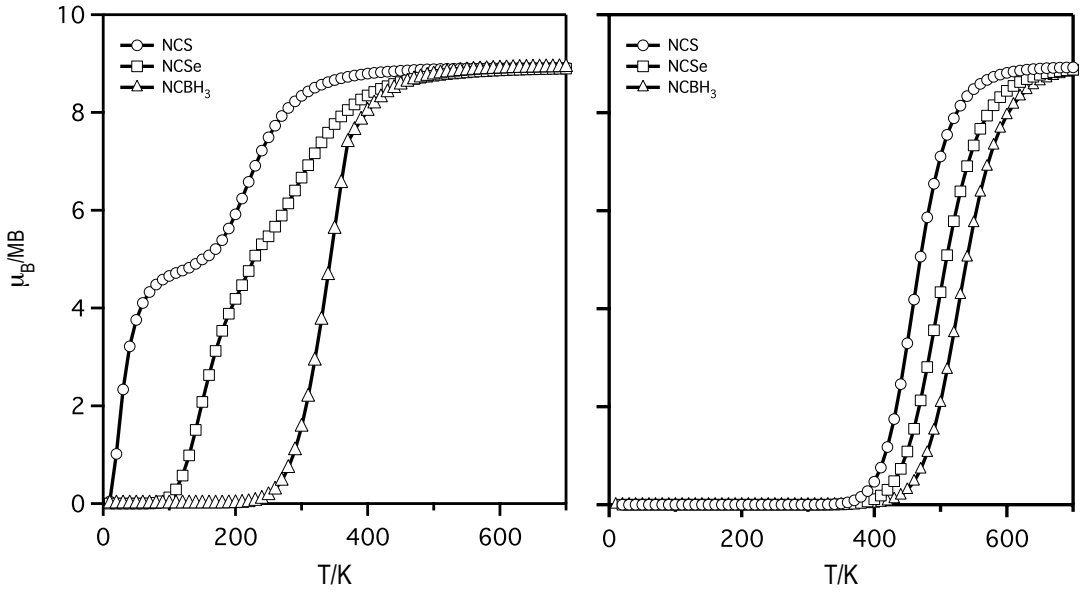

Fig. 5 Calculated magnetic moment for the $[Fe(bt)(NCX)_2]_2(\mu\text{-bpym})$ complexes (**1**-**3**) (left) and $[Fe(pypzH)(NCX)]_2(\mu\text{-pypz})_2$ (right) (**4**-**6**, X = S, Se, BH_3) molecules. Circles for NCS, squares for NCSe and diamonds for $NCBH_3$.

3. Discussion

The rational design of spin-crossover systems with tailored properties is a long pursued goal among the synthetic chemists working in the SCO field. This customized design should also include the possibility of building up dinuclear systems that either exhibit or not a two-step transition via a localized [HS-LS] intermediate spin-state as a function of the specific needs required on the system. A potential approach to this problem is the use of highly constrained ligands that promote the communication between binding pockets.[22-24] However, a disadvantage of this approach is that usually the intermediate [HS-LS] is over stabilized, thus banning the access to the [LS-LS] spin-state. One would expect that if communication between binding pockets is a key step towards the design of dinuclear SCO molecules with a two-step spin-crossover transition, this effect should be somehow reflected in the coordination spheres for the individual metal centers during the different steps of the

transition. Therefore, we would expect some sort of "cooperative" effect for the $[Fe(bt)(NCX)_2]_2(\mu\text{-bpym})$ family (1-3) that should not be present in the $[Fe(pypzH)(NCX)]_2(\mu\text{-pypz})_2$ systems (4-6). A direct analysis of the coordination spheres for the iron(II) centers in our optimized structures for each metal center in all possible spin states shows that, in fact, both systems behave in a similar way seems, however, not to fully agree with this practical approach. A quantitative way to analyze coordination polyhedral is by using Continuous Shape Measures (CShM).[45, 46] The CShM can easily quantify the degree of octahedricity for the metal center and its direct coordination environment, thus providing with an overall quantitative measurement of the corresponding coordination polyhedron (see ESI). A CShM value of zero means that both reference and coordination polyhedral match, and the CShM value will increase with the degree of distortion. However, what we can extract from the CShM analysis is quite the opposite. In the $[Fe(bt)(NCX)_2]_2(\mu\text{-bpym})$ family, when one metal center undergoes SCO, the other metal center remains almost insensitive to that change, as can be seen from the corresponding differences between the CShM in the [LS-LS] and the [HS-LS] spin states (see Table 3). However, larger changes are observed in the $[Fe(pypzH)(NCX)]_2(\mu\text{-pypz})_2$ systems for the same processes, meaning that the communication between the metal centers is more effective, effect that is perfectly understandable on the basis of the ligand pypzH. Therefore, this analysis seems to point out that communication should tend to suppress the two-step transition, and that metal centers that can't talk to each other would be, in principle, more prone to display a two-step transition. Although this changes can be, in fact quantified, in our experience such tiny changes cannot be used as a sole reason to justify the difference behavior between the two series.

Table 3 Calculated Continuous Shape Measures (CShM) with respect to the octahedron for the $[Fe(bt)(NCX)_2]_2(\mu\text{-bpym})$ and $[Fe(pypzH)(NCX)]_2(\mu\text{-pypz})_2$ (X = S, Se, BH_3) molecules. First and second columns for the [LS-LS] spin state, third and fourth column for the [HS-LS] spin state.

System	LS-Fe_1	LS-Fe_2	HS-Fe_1	LS-Fe_2
(**1**) $[Fe(bt)(NCS)_2]_2(\mu\text{-bpym})$	0.50	0.50	2.27	0.50
(**2**) $[Fe(bt)(NCSe)_2]_2(\mu\text{-bpym})$	0.49	0.49	2.14	0.51
(**3**) $[Fe(bt)(NCBH_3)_2]_2(\mu\text{-bpym})$	0.50	0.50	1.91	0.51
(**4**) $[Fe(pypzH)(NCS)]_2(\mu\text{-pypz})_2$	0.59	0.59	1.94	0.64
(**5**) $[Fe(pypzH)(NCSe)]_2(\mu\text{-pypz})_2$	0.59	0.59	1.92	0.64
(**6**) $[Fe(pypzH)(NCBH_3)]_2(\mu\text{-pypz})_2$	0.61	0.61	1.95	0.66

Therefore, we proceed to analyze the underlying electronic structure of the studied systems in terms of the relevant molecular orbitals. A close inspection to the d-based molecular orbital for the metal centers reveals significant differences between the two families. The most striking feature is the energy shift of the $d_{x^2-y^2}$ (see Fig. 6) orbital due different coordination environment of the iron centers in the two families. Thus, in the $[Fe(bt)(NCX)_2]_2(\mu\text{-bpym})$ complexes, such orbital is oriented towards three aromatic aromatic N-ligands and one NCX ligand (which is lower in the spectrochemical series than aromatic N-ligands) while in the $[Fe(pypzH)(NCX)]_2(\mu\text{-pypz})_2$ compounds, there are four aromatic N-ligands in the equatorial coordination. This different coordination environment shifts the energy of the antibonding $d_{x^2-y^2}$ orbital, resulting in a larger energy gap (see Table S4) regardless the fact that d_{z^2} orbital energy remains almost unchanged because the axial coordination is equivalent for the two families of complexes.

Also, it is worth noting that the increasing ligand field strength introduced by the series NCS < NCSe < $NCBH_3$ series can be rationalized on the different π-backbonding character for this series of ligands.[36] Other differences can be found un the low-lying occupied d-based Mos, that can be understood by comparing the corresponding isocontours. The distance Fe-NCS is significantly shorter for the $[Fe(bt)(NCS)_2]_2(\mu\text{-bpym})$ compared to the $[Fe(pypzH)(NCS)]_2(\mu\text{-pypz})_2$ molecule (1.925 Å and 1.953 Å respectively), which points out to a tighter bond between the metal center and the NCS ligand. This is translated in a larger antibonding interaction between the proper p-type orbital of the NCS ligand and the d_{xz}/d_{yz} pair of orbitals, thus making them less non-bonding and increasing its formal antibonding π character. This orbital interaction effectively raises the energy of the d_{xz}/d_{yz} pair of d-based MOs, thus reducing the energy gap between the occupied and empty d-based MOs. Second, the angle Fe-NCS is almost 20º smaller for the $[Fe(pypzH)(NCS)]_2(\mu\text{-pypz})_2$ molecule (150.75º respect an average value of 168.02º), thus reducing the overlap between the suitable p orbital of the NCS ligand and the corresponding metal d_{xz}/d_{yz} orbital. This interaction reduces the antibonding character of the corresponding d-based d-MOs in the $[Fe(pypzH)(NCS)]_2(\mu\text{-pypz})_2$ molecule, thus lowering the energy of the occupied orbitals and increasing the energy gap between them and empty d-based MOs. Finally, the $[Fe(bt)(NCS)_2]_2(\mu\text{-bpym})$ molecule has two NCS ligands in *cis* configuration, which gives the non-bonding d_{xy} orbital a certain antibonding character (see Fig. 6). The same orbital remains purely non-bonding in the $[Fe(pypzH)(NCS)]_2(\mu\text{-pypz})_2$ molecule.

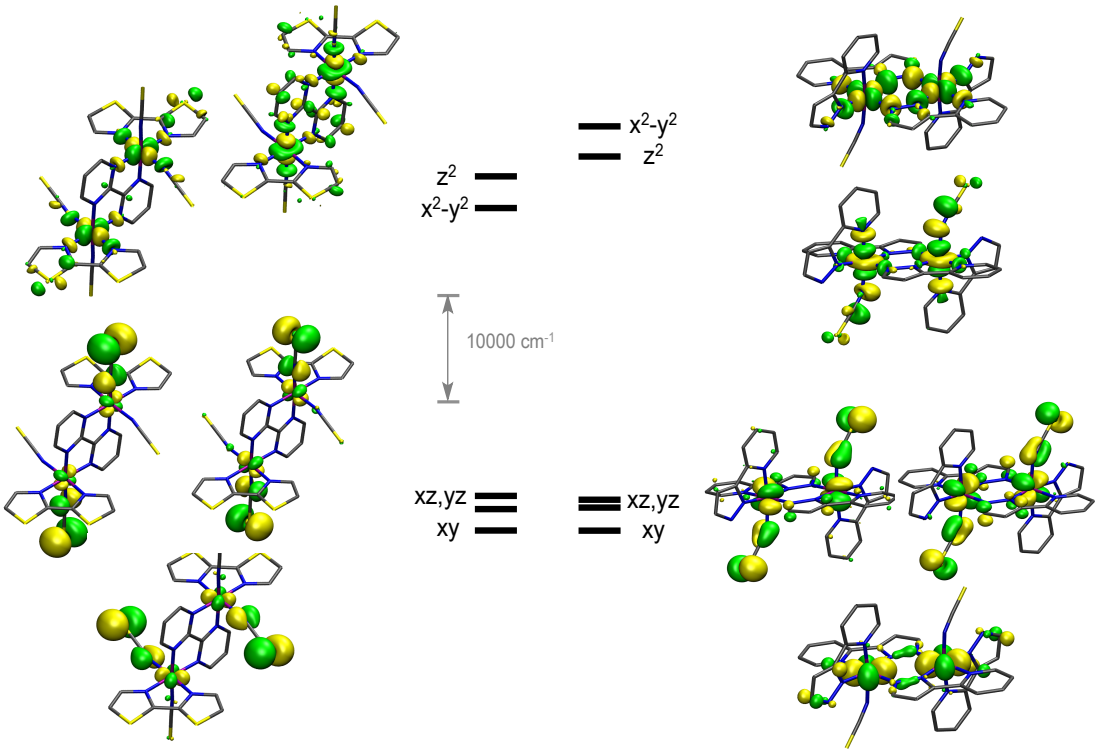

Fig. 6 Isocontours (0.04 e/Å^3) of the d-based molecular orbitals for the [Fe(bt)(NCS)$_2$]$_2$(μ-bpym) (left) and [Fe(pypzH)(NCS)]$_2$(μ-pypz)$_2$ (right) molecules. All energies are in cm^{-1} and referred to the lowest energy d-MO. Hydrogen atoms omitted for clarity.

4. Conclusions

Due to the interest that spin-crossover systems generate, in particular for their potential applications in the design of multifunctional materials, molecular sensors and nanoscale memory devices, accurate molecular level characterization of their electronic properties becomes a very useful tool for the rational design of SCO systems with tailored properties. In this paper, we presented our results for the accurate modeling of the spin-crossover transition in dinuclear iron(II) systems. In particular we applied our previously reported methodology to the [Fe(bt)(NCS)$_2$]$_2$(μ-bpym) and [Fe(pypzH)(NCS)]$_2$(μ-pypz)$_2$ (X=S, Se, BH$_3$) systems, the former displaying a two-step SCO transition and the later a single step sharp SCO transition. The meta-hybrid GGA functional TPSSh, which has been successfully applied to mononuclear Fe^{II} and Co^{II} spin-crossover molecules provides with accurate

calculations of the thermochemical quantities associated with the transition from the [LS-LS] to the [HS-LS] spin-state, and from the [HS-LS] to the [HS-HS] spin-states, quantities that can later be used to extract relative populations of each spin-state as a function of the temperature, therefore allowing for the *in silico* modeling of the spin-crossover curve. Our results are in good agreement with the experimental values, not only in terms of reproducing the shape of the SCO transition but also providing with good quantitative values for the computed transition temperatures. Previous calculations on the $[Fe(bt)(NCS)_2]_2(\mu\text{-bpym})$ and $[Fe(bt)(NCSe)_2]_2(\mu\text{-bpym})$ molecules using the B3LYP* functional, specifically parameterized for mononuclear Fe^{II} SCO systems by adjusting the amount of Hartree−Fock exchange to 15%,[30, 32] also predict the correct sign for the W parameter and progressive destabilization of the [HS-LS] spin-state upon replacing of the NCS ligand by NCSe.[27] However, the reported computed changes in the ΔH are significantly larger than the ones calculated with the TPSSh functional (32% larger) meaning that computing $T_{1/2}$ using the B3LYP* will be subject to larger errors than with the our reported methodology.

A more interesting outcome of the calculations is the fact that the presence or absence of a two-step transition seems to be mostly controlled by the local electronic structures of the metal centers. Small structural changes can be found in the coordination spheres of the metal centers when switching from the [LS-LS] to the [HS-LS] spin state (Table 3). This changes are slightly larger for systems with more constrained ligands ($[Fe(pypzH)(NCX)]_2(\mu\text{-pypz})$, X = S, Se or BH_3) in which communication between binding pockets is more likely to happen, but this changes alone are not enough to justify the different behavior observed in the studied systems. From our results, a much larger contribution arises from the local electronic structures of the Fe^{II} metal centers. Small gaps between the occupied and empty d-based

molecular orbitals lead to a more favorable situation for a two-step spin-crossover to occur, while larger gaps seem to favor a single step transition. Because light chemical modifications on the ligand field can be achieved via chemical modifications, such as the replacement of the NCS ligand by an NCSe or a $NCBH_3$ ligand, it is possible to enhance or reduce the electronic contribution to the two-step transition, thus allowing for a fine tuning control over the physical properties of these dinuclear molecules.

The reported methodology allows for the electronic structure modeling of dinuclear spin-crossover system with accurate prediction of their transition temperatures, and opens the door for a virtual screening of chemical modifications on already existing dinuclear spin-crossover molecules to explore in which way is possible to increase or decrease the stability of the intermediate spin-state, thus allowing for a finer degree of control over the shape of the spin-transition curve. This results set up the first steps towards the *in silico* modeling of polynuclear spin-crossover molecules. Understanding how the transition takes place and which effects are at play in having a given behavior is key in the rational design of spin-crossover materials with selected properties.

Acknowledgments

This research was funded by the Ministerio de Economía y Competitividad through grants CTQ2011-23862-C02-01. J.C. gratefully acknowledges financial support from the Generalitat de Catalunya (Beatriu de Pinós-Marie Curie COFUND Fellowship, 2013 BP-B 00155). E.R. thanks Generalitat de Catalunya for an ICREA Academia fellowship.

References:

1. L. Cambi and L. Szego, *Ber. Dtsch. Chem. Ges.*, 1931, 64, 2591-2598.
2. P. Gütlich and H. A. Goodwin, eds., *Spin Crossover in Transition Metal Compounds I, II and III*, Springer, New York, 2004.
3. A. Bousseksou, G. Molnar, L. Salmon and W. Nicolazzi, *Chem. Soc. Rev.*, 2011, 40, 3313-3335.
4. H. A. Goodwin, *Coord. Chem. Rev.*, 1976, 18, 293-325.
5. P. Gütlich, *Struct. Bond.*, 1981, 44, 83-195.
6. E. König, *Struct. Bond.*, 1991, 76, 51-152.
7. H. Toftlund, *Coord. Chem. Rev.*, 1989, 94, 67-108.
8. M. A. Halcrow, ed., *Spin-Crossover Materials: Properties and Applications*, John Wiley & Sons, Hoboken, 2013.
9. M. C. Muñoz and J. A. Real, *Coord. Chem. Rev.*, 2011, 255, 2068-2093.
10. P. Gütlich, A. B. Gaspar and Y. Garcia, *Beilstein J. Org. Chem.*, 2013, 9, 342-391.
11. Y. C. Chen, Y. Meng, Z. P. Ni and M. L. Tong, *Journal of Materials Chemistry C*, 2015, 3, 945-949.
12. I. Suleimanov, O. Kraieva, J. S. Costa, I. O. Fritsky, G. Molnar, L. Salmon and A. Bousseksou, *Journal of Materials Chemistry C*, 2015, 3, 5026-5032.
13. E. Holmström and L. Stixrude, *Phys. Rev. Lett.*, 2015, 114.
14. E. Ruiz, *Phys. Chem. Chem. Phys.*, 2014, 16, 14-22.
15. M. Ohba, K. Yoneda, G. Agusti, M. Carmen Munoz, A. B. Gaspar, J. A. Real, M. Yamasaki, H. Ando, Y. Nakao, S. Sakaki and S. Kitagawa, *Angew. Chem. Int. Ed.*, 2009, 48, 4767-4771.
16. D. Aravena and E. Ruiz, *J. Am. Chem. Soc.*, 2012, 134, 777-779.
17. A. Lapresta-Fernandez, M. Pegalajar Cuellar, J. Manuel Herrera, A. Salinas-Castillo, M. del Carmen Pegalajar, S. Titos-Padilla, E. Colacio and L. Fermin Capitan-Vallvey, *Journal of Materials Chemistry C*, 2014, 2, 7292-7303.
18. C. Bartual-Murgui, A. Akou, C. Thibault, G. Molnar, C. Vieu, L. Salmon and A. Bousseksou, *Journal of Materials Chemistry C*, 2015, 3, 1277-1285.
19. P. G. Lacroix, I. Malfant, J. A. Real and V. Rodriguez, *Eur. J. Inorg. Chem.*, 2013, 615-627.
20. A. B. Gaspar, M. C. Muñoz and J. A. Real, *J. Mater. Chem.*, 2006, 16, 2522-2533.
21. K. S. Murray, *Eur. J. Inorg. Chem.*, 2008, 3101-3121.
22. M. H. Klingele, B. Moubaraki, J. D. Cashion, K. S. Murray and S. Brooker, *Chem. Commun.*, 2005, 987-989.
23. A. Bhattacharjee, V. Ksenofontov, J. A. Kitchen, N. G. White, S. Brooker and P. Guetlich, *Appl. Phys. Lett.*, 2008, 92.
24. C. M. Grunert, S. Reiman, H. Spiering, J. A. Kitchen, S. Brooker and P. Guetlich, *Angew. Chem. Int. Ed.*, 2008, 47, 2997-2999.
25. J. A. Real, H. Bolvin, A. Bousseksou, A. Dworkin, O. Kahn, F. Varret and J. Zarembowitch, *J. Am. Chem. Soc.*, 1992, 114, 4650-4658.
26. V. Ksenofontov, A. B. Gaspar, V. Niel, S. Reiman, J. A. Real and P. Gutlich, *Chem. Eur. J.*, 2004, 10, 1291-1298.
27. S. Zein and S. A. Borshch, *J. Am. Chem. Soc.*, 2005, 127, 16197-16201.
28. H. Paulsen, V. Schuenemann and J. A. Wolny, *Eur. J. Inorg. Chem.*, 2013, 628-641.
29. M. Reiher, O. Salomon and B. A. Hess, *Theor. Chem. Acc.*, 2001, 107, 48-55.

30. M. Reiher, *Inorg. Chem.*, 2002, 41, 6928-6935.
31. M. Swart, A. R. Groenhof, A. W. Ehlers and K. Lammertsma, *J. Phys. Chem. A*, 2004, 108, 5479-5483.
32. M. Reiher, *Chimia*, 2009, 63, 140-145.
33. V. N. Staroverov, G. E. Scuseria, J. M. Tao and J. P. Perdew, *J. Chem. Phys*, 2003, 119, 12129-12137.
34. J. M. Tao, J. P. Perdew, V. N. Staroverov and G. E. Scuseria, *Phys. Rev. Lett.*, 2003, 91.
35. K. P. Jensen and J. Cirera, *J. Phys. Chem. A*, 2009, 113, 10033-10039.
36. J. Cirera and F. Paesani, *Inorg. Chem.*, 2012, 51, 8194-8201.
37. K. P. Kepp, *Coord. Chem. Rev.*, 2013, 257, 196-209.
38. S. R. Mortensen and K. P. Kepp, *J. Phys. Chem. A*, 2015.
39. B. A. Leita, B. Moubaraki, K. S. Murray, J. P. Smith and J. D. Cashion, *Chem. Commun.*, 2004, 156-157.
40. M. J. Frisch, G. W. Trucks, H. B. Schlegel, G. E. Scuseria, M. A. Robb, J. R. Cheeseman, G. Scalmani, V. Barone, B. Mennucci, G. A. Petersson, H. Nakatsuji, M. Caricato, X. Li, H. P. Hratchian, A. F. Izmaylov, J. Bloino, G. Zheng, J. L. Sonnenberg, M. Hada, M. Ehara, K. Toyota, R. Fukuda, J. Hasegawa, M. Ishida, T. Nakajima, Y. Honda, O. Kitao, H. Nakai, T. Vreven, J. A. Montgomery Jr., J. E. Peralta, F. Ogliaro, M. J. Bearpark, J. Heyd, E. N. Brothers, K. N. Kudin, V. N. Staroverov, R. Kobayashi, J. Normand, K. Raghavachari, A. P. Rendell, J. C. Burant, S. S. Iyengar, J. Tomasi, M. Cossi, N. Rega, N. J. Millam, M. Klene, J. E. Knox, J. B. Cross, V. Bakken, C. Adamo, J. Jaramillo, R. Gomperts, R. E. Stratmann, O. Yazyev, A. J. Austin, R. Cammi, C. Pomelli, J. W. Ochterski, R. L. Martin, K. Morokuma, V. G. Zakrzewski, G. A. Voth, P. Salvador, J. J. Dannenberg, S. Dapprich, A. D. Daniels, Ö. Farkas, J. B. Foresman, J. V. Ortiz, J. Cioslowski and D. J. Fox, Gaussian, Inc., Wallingford, CT, USA, 2009.
41. A. Schäfer, C. Huber and R. Ahlrichs, *J. Chem. Phys*, 1994, 100, 5829-5835.
42. R. Boča and W. Linert, *Monatsh. Chem.*, 2003, 134, 199-216.
43. P. Gütlich, H. Köppen, R. Link and H. G. Steinhäuser, *J. Chem. Phys*, 1979, 70, 3977-3983.
44. J. A. Real, I. Castro, A. Bousseksou, M. Verdaguer, R. Burriel, M. Castro, J. Linares and F. Varret, *Inorg. Chem.*, 1997, 36, 455-464.
45. S. Alvarez, P. Alemany, D. Casanova, J. Cirera, M. Llunell and D. Avnir, *Coord. Chem. Rev.*, 2005, 249, 1693-1708.
46. S. Alvarez and E. Ruiz, in *Supramolecular Chemistry, From Molecules to Nanomaterials,*, eds. J. W. Steed and P. A. Gale, John Wiley & Sons, Chichester, UK, 2012, vol. 5, pp. 1993-2044.